Chinese Journal of Polar Science, Vol. 21, No. 2, 113 - 126, December 2010

Calculation of photosynthetically available radiation using multispectral data in the Arctic

Zhao Jinping(赵进平)[1*], Wang Weibo(王维波)[1] and Cooper Lee[2]

1 Ocean University of China, Qingdao 266100, China

2 Chesapeake Biological Laboratory, University of Maryland, Solomons, MD 20688, USA

** E-mail: jpzhao@ouc.edu.cn*

Received July 30, 2010

Abstract Photosynthetically Available Radiation (PAR) is an important bio-optical parameter related to marine primary production. PAR is usually measured by a broadband sensor and can also be calculated by multispectral data. When the PAR is calculated by multispectral data in polar region, four factors are possible error sources. PAR could be overestimated as the wavelengths of multispectral instrument are usually chosen to evade main absorption zones of atmosphere. However, both PARs calculated by hyperspectral and multispectral data are consistent with an error less than 1%. By the fitting function proposed here, the PAR calculated by multispectral data could attain the same accuracy with that by hyperspectral data. To calculate the attenuation rate of the PAR needs PAR_0, the PAR just under the surface. Here, an approach is proposed to calculate PAR_0 by the best fit of the irradiance profile of 1-5 m with a content attenuation coefficient under surface. It is demonstrated by theory and observed data in different time at same location that the attenuation coefficient of PAR is independent of the intensity of radiation. But under sea ice, the attenuation coefficient of PAR is a little bit different, as the spectrum of the light has been changed by selective absorption by the sea ice. Therefore, the difference of inclusions inside the sea ice will result in different PAR, and impact on the attenuation of PAR. By the results of this paper, PAR can be calculated reliably by multispectral data.

Key words PAR, marine optics, field observation, multispectral, solar radiation.

doi: 10.3724/SP.J.1085.2010.00113

1 Introduction

Photosynthesis is a process by which the plant fixes carbon dioxide and produces dry substance by the action of solar energy. The Photosynthetically Available Radiation (PAR) is the part of the solar energy utilized by chloroplast of the plant for photosynthesis[1]. The main assimilative wavelength is 400—700 nm, about half of the arriving solar radiation energy[2,3]. The spectral domain of PAR is the main scope of the solar radiation through the ocean[4,5]. PAR is an optical parameter mutually in-

teractions with phytoplankton. The spatial distribution of PAR as the energy source of primary production influences the reproduction of the phytoplankton. On the other hand, the distribution of the phytoplankton changes the absorption of light in the seawater, which in turn influences the vertical distribution of PAR[6,7]. The profiling of the PAR is used to reveal the intensity of PAR in different levels, and the data is benefit to study the vertical distribution of the algae and primary production[8]. The main components in the atmosphere to absorb the solar radiation in the scope of 400—700 nm are oxygen and ozone, basically independent to the vapor and CO_2[9]. In the ocean, PAR is mainly influenced by phytoplankton. As the species of phytoplankton in different region are not the same, the spectral component of PAR becomes regionally distinct[1].

PAR sensor is usually optical ones with broadband to receive the light in the scope of 400—700 nm, which could be used alone or with the other instrument system[10]. Besides, the spectral data could be integrated to calculate PAR. The spectral data includes multi-spectral and hyperspectral data. The hyperspectral instruments are prismatic to gain the hundreds of spectral data which is with narrow bands and covers all of the wavelengths. The numerous bands are benefit to calculate PAR to gain the same spectral response of the broadband sensors[11]. However, the spectral instruments with the multi-sensors and filters are usually equipped with some selected wavebands to fit the atmospheric transmission window to avoid the absorption zones. The multi-spectral instruments are with high sensitivity to facilitate the optical measurement for weak light in deeper ocean[12], but it might bring errors by their limited wavebands. There are three significances to calculate PAR by multi-spectral instruments. Firstly, the successful calculation of PAR by multi-spectral data increases the datasets of PAR in favor of the ecological study. Secondly, the use of the PAR sensor usually is not calibrated by the surface measurement, and the PAR underwater recorded cannot exclude the impact from the cloud, fog, and the other factors to cause the change of PAR during measurement. Whereas the underwater multi-spectral data are well corrected by the simultaneous observation on the surface, and the calculated PAR might be more reliable. Thirdly, the multi-spectral data can be used to find out the components of PAR in different wavebands, which is benefit to reveal the action of PAR on the different species of phytoplankton with separate absorption abilities. Morel and Smith (1974) defined the three kinds of water types by the wavelength λ_{Hmax} at the maximum intensity at specific depth of the sea. The first type of water is blue water, and the scope of the λ_{Hmax} is 440—475 nm. The Type II water is blue-green color with the λ_{Hmax} in 475—515 nm. The Type III water is green water with λ_{Hmax} beyond 515nm. The sensitive connection of spectral instruments and the phytoplankton enable us to reveal the spectral components of PAR in different types of water.

The sensors in multi-spectral instrument are usually not enough. For example, there are 18 wavebands in the Profiling Reflectance and Radiometer system (PRR-800) with the bandwidth of 10 nm. It covers 180 nm, one third of 400—700 nm is not covered[13], which would bring some error if it is used to calculate the PAR by interpolation. The waveband of the instrument is always chosen to avoid the absorption

zone of atmosphere, which might overestimates the calculated PAR and the irradiance needs to be calibrated before using.

In the polar region, the arriving solar radiation is quite different from that in mid-latitude. Under the very low solar altitude condition, the arriving PAR down to the surface decreases by the longer light path, thicker optical thickness, and increased vapor absorption[14]. The ice cover will impact strongly on the measured result. These issues will be discussed in detail in this paper to provide the solution theoretically and applicably for PAR calculation.

2 The applicable theory to calculate PAR by multi-spectral data

There are two kinds of measurements of PAR, for scalar irradiance and cosine irradiance. The response of biomass for light during photosynthesis is mainly a scalar irradiance in which only the radiation intensity is considered, independent of the direction of incident light. Thus, PAR is defined as the integral of the radiance for spherical solid angle of 4π, i. e. links to

$$\int_{4\pi} L(\theta,\varphi,\lambda)d\Omega \tag{1}$$

Where L is the radiance with the unit μW cm^{-2} • nm^{-1} • sr^{-1}; Ω is the solid angle, θ and φ is the zenith and azimuth of the radiance flux. The other is cosine irradiance, which is measured by a sensor with the flat quantum response. The response of the sensor is proportional to the cosine of the zenith, similar to the radiation arriving at a plant on a horizontal plane, i. e. links to

$$\int_{4\pi} L(\theta,\varphi,\lambda)\cos\theta d\Omega \tag{2}$$

Therefore, one must know what kind of instrument or PAR is used. The under water sensors for PAR measurement are usually flat quantum response ones, which will be discussed in this paper.

According to the definition of the optics, the integral of radiance for the 2π space is called as the downwelling irradiance[15].

$$E_d(\lambda) = \int_{2\pi} L(\theta,\varphi,\lambda)\cos\theta d\Omega \tag{3}$$

The unit of E_d is the unit of flux W • m^{-2} • nm^{-1} or J • m^{-2} • s^{-1} • nm^{-1}。

PAR has two kinds of computation systems. One is the energy system, which is integrated directly by E_d. The other is quantum system to calculate the photosynthetically quantum flux density with the unit of mol • m^{-2} • s^{-1}[16]. The conversion between them is: photons per Mole is the Avogadro number ($A_v = 6.02\times10^{23}$ photon • mol^{-1}); $A_v\times$PAR(λ) is the photons arriving at unit area per unit time. The energy of a photon is $e=hc/\lambda$, where h is the Planck number ($=6.63\times10^{-34}$ J • s), c is the velocity of light, and λ is the wavelength of light. Therefore, the total energy per unit area and time (J • m^{-2} • s^{-1} • nm^{-1}) of the light with the wavelength λ can be expressed as

$$\frac{A_v hc\,\mathrm{PAR}(\lambda)}{\lambda} = E_d(\lambda) \tag{4}$$

Integral for the scope of 400—700 nm, the PAR could be calculated by

$$\mathrm{PAR} = \int_{400}^{700} \mathrm{PAR}(\lambda)d\lambda = \frac{1}{A_v hc} \int_{400}^{700} \lambda E_d(\lambda)d\lambda \tag{5}$$

The unit of PAR is μmol • m^{-2} • s^{-1}, or μE • m^{-2} • s^{-1}.

It is implies from Eq. (5) that the precision of PAR calculation is mainly related to the measured irradiance. Otherwise, there are some factors regarding the radiation spectrum and shining condition might influence the accuracy of calculated PAR, which will be discussed in detail in this study.

3 The error and calibration of PAR calculated by multi-spectral data

Owing to the wavebands of the multi-spectral instruments is always selected to evade the spectral absorption zones of atmosphere, the calculated PAR integrated by the irradiances within 400—700 nm could be overestimated. The main issue using multi-spectral data to calculate PAR is the error level and the efficiency of its calibration. The PAR calculated by hyperspectral data are adopted as a standard to compare with the PAR calculated by multi-spectral data. First, the hyper-spectral data are used to obtain PAR. Then, the eighteen wavebands corresponding to the multi-spectral instrument are sought out to calculate PAR again. The error is estimated from both PARs.

The hyper-spectral instrument is Profiler-II produced by Satlantic Inc., which is used to measure water irradiance in the July of 2008 during the ninth cruise of Canadian "Circumpolar Flaw Leads Study (CFL)" program. Twelve wavebands that are corresponding to the wavebands of PRR-800 are selected from the 89 wavebands in the scope of 400—700 nm. They are 412, 443, 490, 510, 520, 532, 555, 565, 589, 625, 665 and 683 nm. The different coverage of the multi-and hyper-spectral data is plotted in Fig. 1.

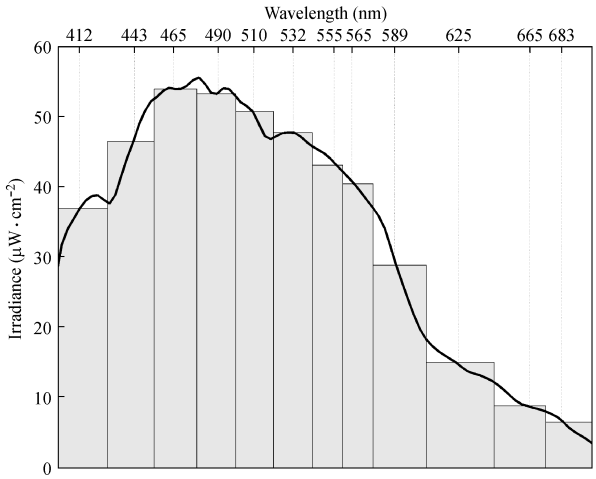

Fig. 1 Different coverage of multispectral and hyperspectral data. Curve denotes the hyperspectrum measured by Profiler-II, and the histogram denotes the multispectrum selected by PRR-800.

We first calculate PAR by Eq. (5) using the hyper-spectral data in the scope of 400-700 nm. The calculated PAR is completely consistent with the PAR the instrument provided by the same algorithm. Then, the data for the twelve wavebands are used to calculate PAR to find out the difference between them. Let subscript i denotes the result of multi-spectral data and k denotes the result with hyper-spectral data, the Eq. (6) comes into existence in a width of a multi-spectrum band.

$$\alpha_i \lambda_i E_{di} \Delta\lambda_i = \sum_k \lambda_k E_{dk} \Delta\lambda_k \quad (\Delta\lambda_i = \sum_k \Delta\lambda_k) \tag{6}$$

The parameter α_i is used to express the difference of PAR calculated by multi- and hyper-spectral data. Eq. (5) could be change to as

$$\int_{400}^{700} \lambda E_d(z,\lambda) d\lambda \approx \sum_k \lambda_k E_{dk} \Delta\lambda_k = \sum_i \alpha_i \lambda_i E_{di} \Delta\lambda_i \tag{7}$$

The α_i, is related to the choice of wavebands, an instrument-dependent parameter, which is difficult to calculate by Eq. (7) as $\Delta\lambda_i$ might not nicely equals to the sum of $\Delta\lambda_k$. Therefore, the average a, possibly a depth-dependent parameter, is chosen to replace α_i by

$$\alpha = \frac{\sum_k \lambda_k E_{dk} \Delta\lambda_k}{\sum_i \lambda_i E_{di} \Delta\lambda_i} \quad (400\ \text{nm} \leqslant \lambda \leqslant 700\ \text{nm}) \tag{8}$$

The data in clear water should be chosen to calculate α by Eq. (8) to gain a result with larger depth to attain a better calibration.

Eight profiles data of the CFL cruise are used to estimate α in Fig. 2. The maximum relative error is less than 0.01. The results could be fitted for two segments (1—11 m and 11—30 m) by quadratic functions for the whole depth by the least squares method.

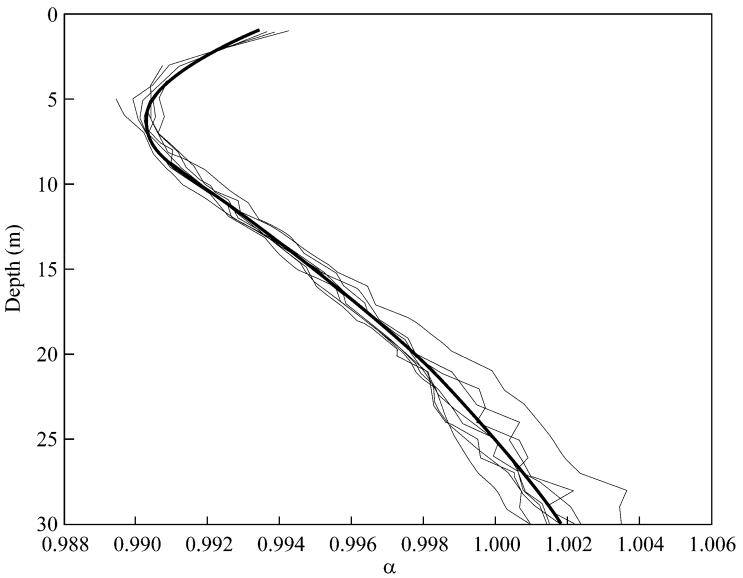

Fig. 2 Vertical profile of α. Measured α at eight stations of CFL cruise(thin line) and fitting result by Eq. (9).

$$\alpha_u = 0.9947 - 0.0014z + 1.1292 \times 10^{-4} z^2$$
$$\alpha_d = 0.9839 + 8.8308 \times 10^{-4} z - 9.4936 \times 10^{-6} z^2 \quad (9)$$

Calculated by multi-spectral irradiance data, simply by multiplying PAR with α. The α depends mainly on the choice of the wavebands, and might be little difference in different regions.

4 Determination of the surface PAR and the attenuation coefficient

When the PAR is acquired, the attenuation coefficient of PAR can be calculated by the Ocean Optics Protocols of NASA[17], which is expressed by

$$\mathrm{PAR}(z) = \mathrm{PAR}(z_m)\exp[-k_m(z - z_m)] \quad (10)$$

The attenuation coefficient varied with depth by the least squares method is

$$k_m = \frac{\sum (z - z_m)\ln[\mathrm{PAR}(z)/\mathrm{PAR}(z_m)]}{\sum (z - z_m)^2} \quad (-4\ \mathrm{m} \leqslant z \leqslant +4\ \mathrm{m}) \quad (11)$$

Based on Eq. (11), the vertical attenuation depth, a depth when the PAR becomes γ percentage could be found out. The calculation is quite simple, but the PAR_0, the PAR just under the sea surface must be accurately determined. If the error for PAR_0 is expressed by $\Delta\mathrm{PAR}_0$, the depth to be determined will have an error of Δz. From Eq. (10),

$$\Delta\,\mathrm{PAR}(z) = -k_m \mathrm{PAR}(z)\Delta z \quad (12)$$

When taking $\mathrm{PAR}(z) = \gamma\mathrm{PAR}_0$, the error of the attenuation depth becomes,

$$\Delta z = -\frac{1}{k_m}\frac{\Delta\,\mathrm{PAR}_0}{\mathrm{PAR}_0} \quad (13)$$

Eq. (13) indicates the following issues. (1) The error for attenuation depth will increase when the bias of PAR_0 increases. (2) The error for attenuation depth will be larger when the water is clear with a smaller k_m. (3) The error for attenuation depth is proportional to the relative error of PAR_0. When the PAR_0 is larger in the clear day, the depth error to be determined will be smaller as the relative error of PAR_0 becomes smaller. The error of the attenuation depth will be larger in the cloudy day or at the morning and evening. For example, if the attenuation coefficient is 0.06, the relative error of PAR_0 is 30%, the error of attenuation depth will be 5 m.

However, the real PAR_0 entering the sea surface is difficult to determine. The surface unit of the instrument measures the PAR arriving onto the sea surface, but most arrived PAR does not enter the ocean, part of them returns to the space. The albedo, the reflected PAR might be helpful to solve the problem, but ships usually do not equipped with albedo sensor as the albedo is difficult to measure from a ship condition by the impact of ship hull. And also the incident irradiance recorded by the surface unit is sometimes quite different from that recorded by underwater unit as the illumination for both units might be inconsistent, especially in the case to deploy the underwater unit from a hole of ice. Therefore, the PAR_0 nearly can not depend on the surface unit, but only on the underwater PAR data itself.

The PAR_0 calculated by the irradiance under surface within several meters is strongly interfered by the waves[11]. Sometimes, PAR_0 is extrapolated from the PAR

in 5—10 m under the sea surface. Usually the extrapolation produces great errors as it attenuated exponentially. The near surface attenuation coefficient could be extrapolated by Eq. (11) under 4 m, and then the PAR_0 could be calculated by Eq. (10). But the attenuation coefficient extrapolated based on the data under 4 m might not suit the surface situation, as the biological activity on the upper several meters may cause stronger attenuation[1].

In view of the advantage of the possible methods, we decide to calculate PAR_0 by the attenuation coefficient of PAR in a smaller depth. Adjusting the depth scope to as $1\ \text{m} \leqslant z \leqslant 5\ \text{m}$ in Eq. (11), k_0 is confirmed to be the vertical attenuation coefficient in the near surface level. Then, PAR_0 is obtained by the least squares method as

$$PAR_0 = \left(\prod_{i=1}^{5} PAR_i\right)^{1/5} \exp(3k_0) \tag{14}$$

The PAR_0 calculated by Eq. (14) is shown in Fig. 3, in which the PAR_0 links well with the PAR in the upper layer water. PAR_0 is a physical parameter that is estimated by various methods and cannot be examined by field experiment in a rough sea condition. It is still impossible to indicate which method is the best one. However, if the attenuation coefficient in the upper ocean could be supposed as a constant, the obtained PAR_0 by the least squares method of Eq. (14) should be the optimal.

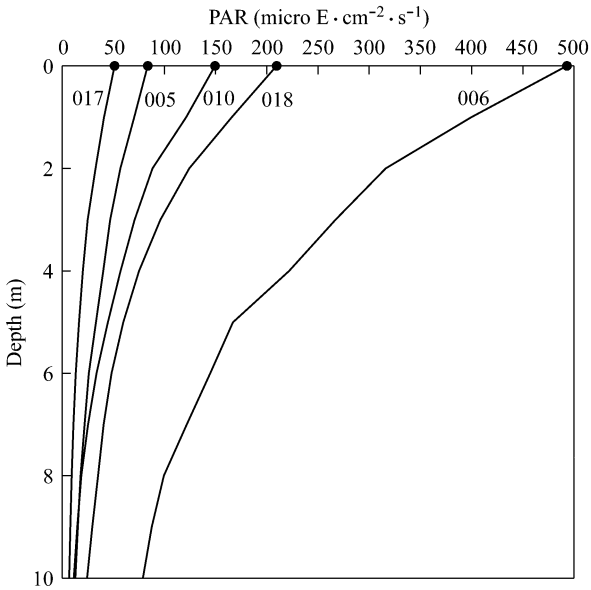

Fig. 3 PAR_0 calculated by multispectral data of Bering Sea cruise in 2008. Numbers are the station numbers and dots indicate the estimate.

Based on the estimation for PAR_0, the attenuation depth of PAR can be calculated by Eq. (13). Fig. 4 shows the depths when PAR attenuated to 50%, 30%, 12%, 5%, and 1% according to the demand of the ecological study during the Bering Sea cruise in 2008 spring, showing the difference in different locations.

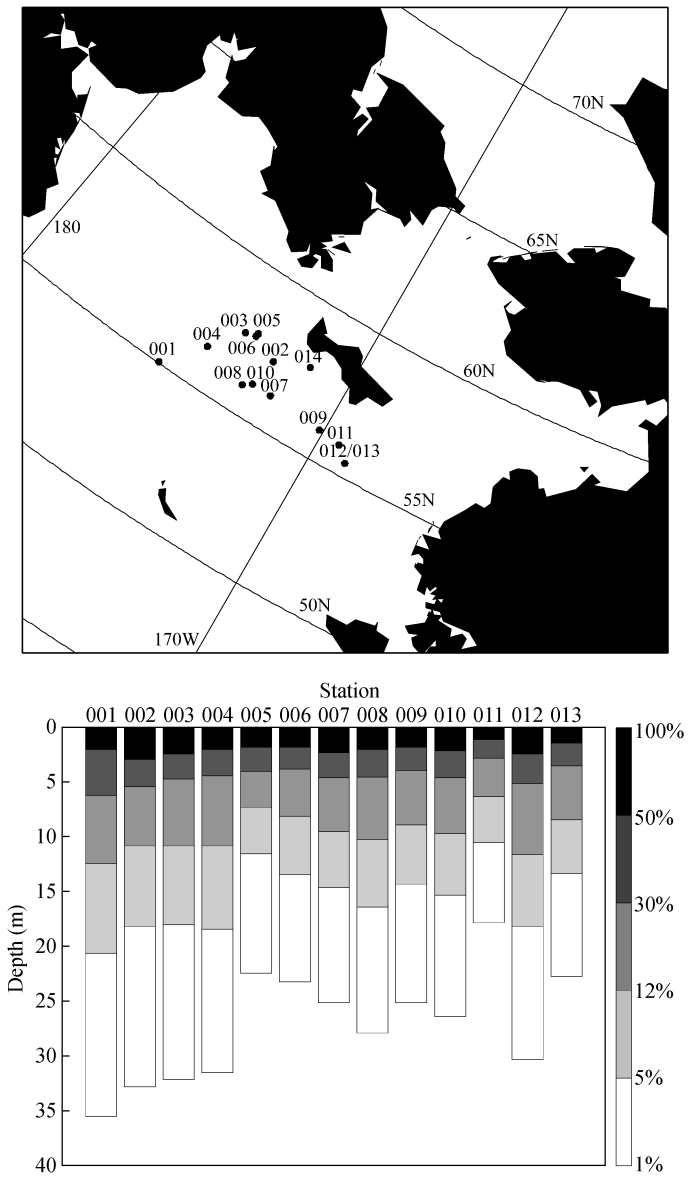

Fig. 4 Attenuation depths of PAR. Upper figure is the thirteen stations during the Bering Sea cruise of 2008, and the lower figure shows the attenuation depths of PAR at the levels of 50%, 30%, 12%, 5% and 1%.

5 Influence of radiation condition on the observed PAR

The value of the PAR is changing with intensity of the incident radiation, but the attenuation coefficient of PAR calculated by Eq. (11) should be determined by the optical property of the seawater, independent of intensity of the incident radiation. In such a way, the attenuation coefficient of PAR could be applied to estimate accurately the photosynthesis in the ocean. The influence of the radiation variation on

the attenuation coefficient of PAR can be estimated theoretically by differential of Eq. (11),

$$\Delta k_m = \frac{1}{\sum (z - z_m)^2} \sum (z - z_m) \left[\frac{\Delta \mathrm{PAR}(z)}{\mathrm{PAR}(z)} - \frac{\Delta \mathrm{PAR}(z_m)}{\mathrm{PAR}(z_m)} \right] \tag{15}$$

Substituting Eq. (10) into Eq. (15), it can be seen that $\Delta k_m = 0$ always exists, which illustrates the attenuation coefficient as an optical property of seawater is independent of the solar radiation.

The variation of the attenuation coefficient of PAR with solar radiation could be acquired by repeated observation at a same place. But the repeated observations are rare as limited ship time. Even if there are such opportunities, error arisen from the ship drifting might not be neglected. Two repeated measurements in Canadian Basin are shown in Fig. 5: one was at Station CB5BR (75°27.66′N, 156°17.11′W) of 2006 and the other was at Station CB-4 (5°00.28′N, 149°59.61′W) of 2009, with the time intervals of 4.8 and 2.5 hours, respectively. The intensity of PAR during the first cast increased at 7 m depth arisen by sea ice shading, but impacted little on the attenuation coefficient (Fig. 5a). In Fig. 5b, the attenuation coefficient somehow appeared wavelike swing in vertical direction, possibly because of the ship drifting or over weak light. However, the average value was close to that of the first cast. It is verified that the varying intensity of PAR from changing radiation exerts little influence on the attenuation coefficient of PAR.

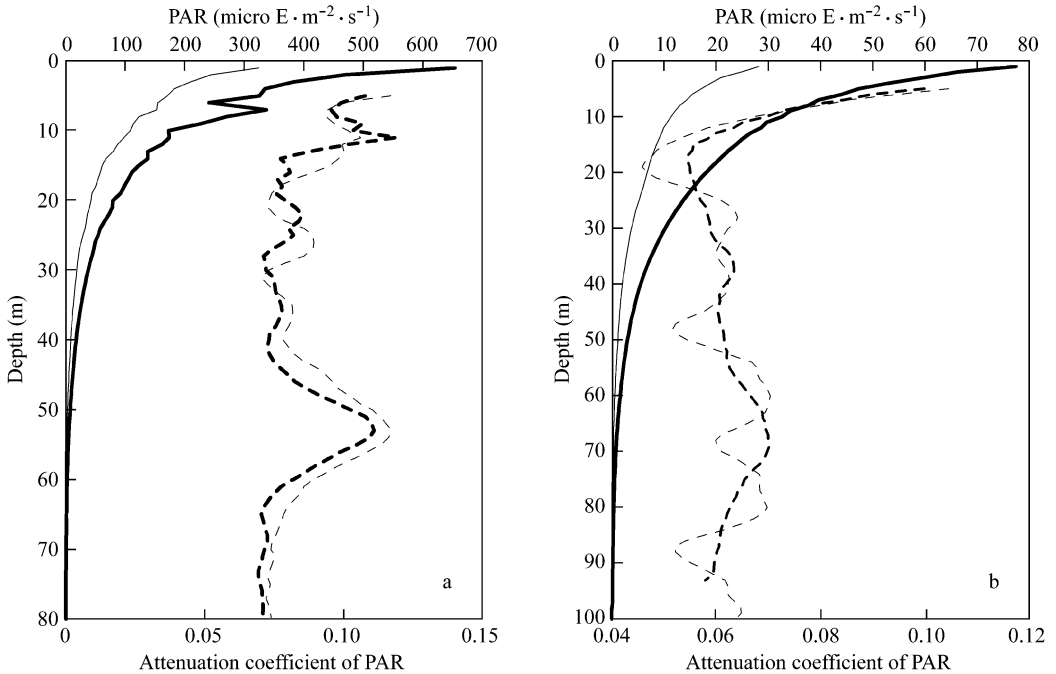

Fig. 5 PAR and its attenuation coefficients measured at different time. (a) Observations at Station CB5BR(75°27.66′N, 156°17.11′W) with the interval of 4.8 hrs; (b) Observations at Station CB-4 (75°00.28′N, 149°59.61′W) with the interval of 2.5 hrs. Thick and thin lines are the results from the first and second casts, respectively. Solid lines denote measured PAR, and dashed lines are the attenuation coefficient of PAR.

The theoretical solution (Eq. 15) and observed results (Fig. 5) all support such a conclusion that the attenuation of PAR is close to an optical property of seawater, controlled by the inclusions in the water and nearly independent of the illumination condition. This conclusion sometime is instructive for the field observation. We could observe the irradiance no matter what the light condition is, such as the direction of incident light, the shading by cloud, fog or ship.

6 Influence of sea ice on PAR

In ice covered situation, the optical observation is usually conducted in a piece of emerging open water cut by ship. The measured irradiance in fact is not the radiation entered into the seawater under ice covered condition. One may ask that can the attenuation of PAR calculated by the newly entered solar radiation represent the ice covered situation. Or, in another words, can the attenuation coefficient measured in factitiously opened water represent the real attenuation when ice covered? Thereby, a comparison is necessary to measure one cast from the ship through emerging open water and the other cast from an ice hole for ice covered water in the same location. It is difficult to find out such data as the observation is quite rare for two casts through ice and ship in the same station.

On the station MK10 during a cruise on Bering Sea in March of 2008, we conducted an optical observation on the ice at 23:33 (UTC) of March 22, and then returned to the ship to conduct another observation on the ship at 02:31 (UTC) of March 23. The movement of the ship within three hours was neglectable. The comparison between the two casts of PARs is plotted on Fig. 6. The under ice PAR was measured through 0.68 m ice and 0.04 m snow, and the light through the attenuation of sea ice was weak. The time for ship observation was close to the evening, so the PAR was weak, but little bite stronger than that under sea ice. The two attenuations were little bit different with a relative error of 12%, the attenuation measured from the ship was weaker.

The main cause to generate the relative error was sea ice that reduced the solar radiation spectrally. The attenuation of sea ice for the solar radiation is[18]

$$E_d = (1-\alpha)E_{d0}\exp(-\delta h) \tag{16}$$

where h is ice thickness. The downwelling irradiance E_{d0} and the spectral albedo α were observed through the surface unit, and the transmission irradiance E_d through sea ice were measured by a under ice instrument. The attenuation coefficient δ of solar radiation through sea ice is

$$\delta = -\frac{1}{h}\ln\left[\frac{E_d}{(1-\alpha)E_{d0}}\right] \tag{17}$$

The spectral attenuation coefficient through sea ice is plotted in Fig. 7. The attenuation of sea ice for solar radiation is selective, obviously attenuated in the waveband greater than 600 nm, which changes the solar spectrum arriving under sea ice[19]. Otherwise, the attenuation coefficient in the figure is about 3.5 m^{-1}, much greater

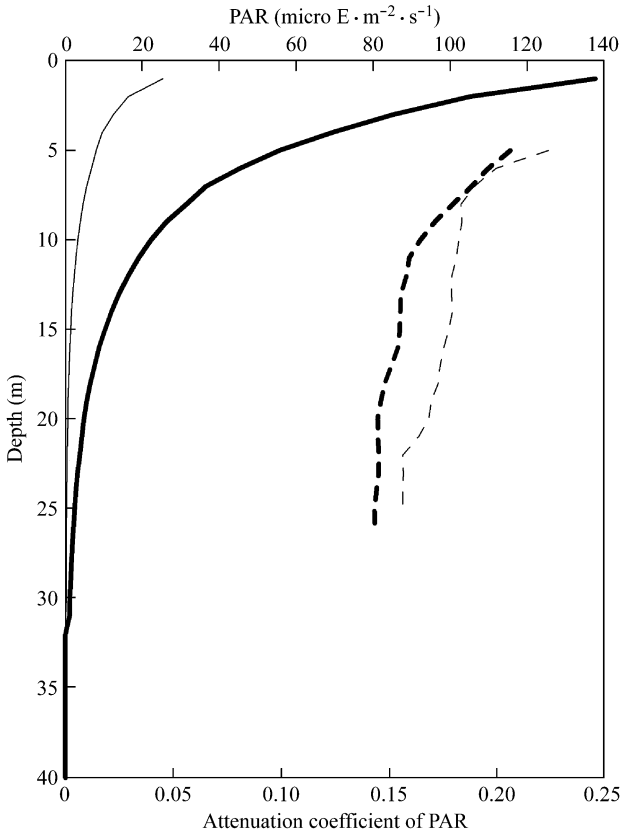

Fig. 6 Observed results on ship (thick solid line) and on ice (thin solid line) at Station MK10 (62°11.57′ N, 169°00.56′W) on the Bering Sea 2008. Solid lines are measured PAR and the dashed lines are the attenuation coefficient of PAR.

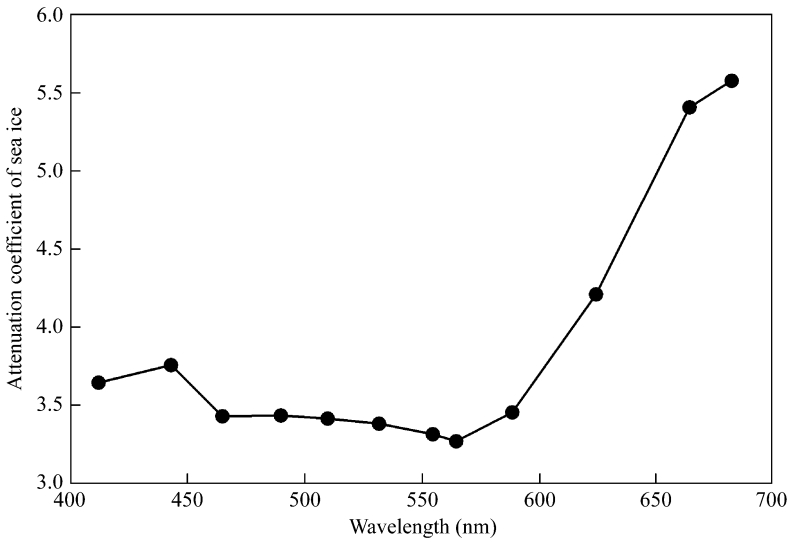

Fig. 7 Spectral attenuation coefficient of sea ice for solar radiation calculated by Eq. (17).

than that of 1.6 m^{-1} we usually use[20], because of the ice algae attached at the base of the ice, which weakens the solar radiation penetrating the sea ice[21]. As a comparison, the sea ice on the Bohai Sea contains many particles forming by suspended dust, which strongly attenuates the light of 400-500 nm[22]. Therefore, the component of PAR changes after penetrating through various sea ices.

As illustrated in Section 5, the difference of PAR produced by radiation intensity should not impact the attenuation of seawater. But when the arriving radiation spectrum alters, the attenuation coefficient of PAR will change accordingly, as the attenuation of water for each wavelength is different. Therefore, the attenuation of PAR in the emerging open water is usually different with that in ice covered water. The higher attenuation coefficient in the ice covered water is postulated to cause by the changing spectrum of penetrated solar radiation. Depending on the unique pair of data, it is impossible to indicate sufficiently the difference of PARs in newly opened water and under sea ice. More observations and studies are necessary in the future.

7 Results and discussion

Photosynthetical available radiation (PAR) is an important bio-optical parameter, which is connected with the primary production process of marine phytoplankton. PAR could be measured directly by the sensor with single waveband, and could be also calculated by multi- or hyper-spectral data. The multispectral data can be used not only for the calculation of PAR, but also to reveal the main spectral components of PAR. Four factors that might produce the calculating error of PAR is studied in this study to ensure the multi-spectral irradiance data to be an reliable data source of PAR.

Owing to the selected spectrums of multi-spectral sensors avoid the main atmospheric absorption zones, the calculated PAR might be overestimated. In this study, the PARs calculated by multi- and hyper-spectral data are verified to approach each other with the relative error less than 1%. Based on the observations in Arctic Ocean, two quadric functions are built to calibrate the calculated PAR by multi-spectral data to attain the similar accuracy with that using hyper-spectral data.

The PAR just under the sea surface, PAR_0, is not measurable in rough sea condition, but is necessary for calculation of the attenuation coefficient. An approach is proposed in this study to calculate the near surface attenuation coefficient first, which is supposed to be a constant, and then to calculate the value of PAR_0 by the least squares method using the observed PAR at 1—5 m. The acquired attenuation coefficient is the optimal estimation of the PAR_0 and connects well with the under water PAR.

The observed PAR data in the same location but different time indicates that the PAR is quite different with the distinct solar altitude. However, the relative error of the attenuation coefficient of PAR is quite small showing that PAR is close to an optical property of seawater, nearly independent of the radiation intensity. Based on this conclusion, the same PAR could be obtained in different time under distinct shining conditions.

Under the ice covered ocean, the ship measured PAR by the newly opened water is not the one really enters into the water, which is different with the PAR directly measured on the sea ice by a hole. Because of the selected absorption of sea ice for the penetrated solar radiation, the component of PAR alters and the attenuation coefficient will change accordingly. Therefore, the sea ice will eventually influence the component of irradiance and the attenuation of PAR.

Via the analysis for calculating PAR by multi-spectral data in polar region, the problems we faced have been studied. It allows us to calculate PAR from multi-spectral data and studies the spatiotemporal variation of PAR in the ice covered region.

Acknowledgements This study was supported by the National Natural Science Foundation of China (Grant No. 40631006) and the China's IPY Program. We are greatly appreciated Prof. Jackie Grabmier of the University of Maryland, Prof. David Barber of the University of Manitoba and Prof. Eddy Carmack of the Institute of Ocean Sciences. Thanks the captains and crews of Healy, Amundsen, and Louis S. St. Laurent icebreakers for their memorable helps.

References

[1] Morel A and Smith RC(1974): Relation between total quanta and total energy for aquatic photosynthesis. Limnology and Oceanography, 19: 591 – 600.

[2] Alados I, Foyo-Moreno I, Alados-Arboledas L (1996): Photosynthetically active radiation measurements and modeling. Agricultural and Forest Meteorology, 78: 121 – 131.

[3] Ross J and Sulev M(2000): Sources of errors in measurements of PAR. Agricultural and Forest Meteotology, 100:103 – 125.

[4] Glover HE, Smith AE, Sharpiro L(1985): Diurnal variations in photosynthetic rates: comparison of ultrophytoplankton with a larger phytoplankton size fraction. J. Plank. Res., 7: 519 – 535.

[5] Jiao NZ and Wang R (1994): Dynamics of marine primary production and the structure of products. Acta Oceanologica Sinica, 16, 85 – 91(in Chinese with English abstract).

[6] Hansen GA, Eilertsen HC, Hegseth EN, *et al*. (1993): On the submarine light field in a phytoplankton model, SPIE., 48(2): 168—174.

[7] Marra J, Barber RT, Trees C, *et al*. (1997): Primary production and irradiance during an intermonsoon cruise to the Arabian Sea (November, 1995), SPIE., 963(2):302 – 307.

[8] Jitts HR, Morel A and Saijo Y(1976): The relation of oceanic primary production to available photosynthetic irradiance. Australian Journal of Freshwater Research, 27:441 – 454.

[9] Kirk JTO(1994): Light and photosynthesis in aquatic ecosystems. Cambridge University Press, 27 – 28.

[10] Glenn SM, Dickey TD, Parker B, *et al*. (2000): Long-term real-time coastal ocean observation networks. Oceanography, 13(1):24 – 34.

[11] Zhao QH, Qin BQ, Zhang YL (2007): the characteristics of the under water light field in the Meiliang Bay of the Lake Tai,. Journal of the optics, 27(5):760 – 765 (in Chinese with English abstract).

[12] Iluz D, Dishon G, Capuzzo E, Meeder E, Astoreca R, Montecino V, Znachor P, Ediger D, Marra J (2009): Short-term variability in primary productivity during a wind-driven diatom bloom in the Gulf of Eilat (Aqaba). Aquatic Microbial Ecology, doi: 10.3354/ame01321, 56: 205 – 215.

[13] Zhao JP, Li T (2010): Solar radiation penetrating through sea ice under very low solar altitude. Journal of Ocean University of China (Oceanic and Coastal Sea Research), DOI 10.1007/s11802-010-0116-7, 116 – 122.

[14] Baker KS(1987): Relation between photosynthetically available radiation and total insolation at the ocean surface under clear skies. Limnol. Oceanogr., 32(6): 1370 - 1377.

[15] Mobley CD(1994): Light and Water: Radiative Transfer in Natural Waters. Academic Press, San Diego, 592.

[16] Cao WX and Yang YZ (2002): the calculation model for the distribution of marine photosynthetical available radiation. Journal of Tropic Oceans, 21(3):47 - 54(in Chinese with English abstract).

[17] Mueller JL, Fargion GS(2003): Ocean Optics Protocols for SeaWiFS Validation, Revision 4. NASA/TM-2003-21621, Greenbelt, Maryland: NASA Goddard Space flight center, 308.

[18] Perovich, DK (1996): *The Optical Properties of Sea Ice*, Monograph 96-1, US Army Corps of Engineers. Cold Regions Research & Engineering Laboratory.

[19] Zhao JP, Li T, Zhang SG, *et al*. (2009): The shortwave solar radiation energy absorbed by packed sea ice in the central Arctic. Advances in Geosciences, 24(1):34 - 42 (in Chinese with English abstract).

[20] Maykut G and Grenfell TC(1975): The spectral distribution of light beneath first-year sea ice in the Arctic Ocean. Limnol. Oceanogr., 20(4): 554 - 563.

[21] Alexander V and Niebauer HJ(1981): Oceanography of the eastern Bering Sea ice-edge zone in spring. Limnol. Oceanogr., 26(6):1111 - 1125.

[22] Qu P, Zhao JP, Li SJ, *et al*. (2009): Spectral solar radiation under sea ice in the Bohai Sea. Acta Oceanologica Sinica, 31(1):37 - 43(in Chinese with English abstract).